Kinetics, isotherms, and thermodynamic studies of Cu (II) adsorption on titanium oxide nanotubes

Bochra Bejaoui Kefi [1, 2, *], Imen Bouchmila [1], Sidrine Koumba [3], Patrick Martin [3, *] and Naceur M'Hamdi[4]

[1] National Institute of Research and Physico-chemical analysis, Laboratory of Useful Materials, Technopark Sidi Thabet, Ariana 2020, Tunisia

[2] Carthage University, Faculty of Sciences, Chemistry Department, 7021, Zarzouna, Bizerte, Tunisia

[3] Unité Transformations & Agroressources, ULR7519, Université d'Artois - UniLaSalle, 62408 Bethune, France

[4] Research Laboratory of Ecosystems & Aquatic Resources, National Agronomic Institute of Tunisia, Carthage University, Tunis, 1082, Tunisia

Abstract: In the present work, titanium oxide nanotubes (TON) were synthesized at the nano-size using the alkaline hydrothermal method and then used to remove Cu(II) ions, by adsorption, from water. The kinetic study of the adsorption of Cu (II) cations on titanium oxide nanotubes was carried out to estimate the amount adsorbed as a function of time and determine the time for maximum adsorption. The results showed that the kinetic equilibrium is reached after a time that increases with the initial concentration of Cu(II). The kinetics and isotherm are studied, considering the effects of different parameters (initial concentration, contact time, pH, and temperature). The pseudo-second-order model perfectly described the adsorption kinetics over the whole concentration range studied. The equilibrium data revealed that the Langmuir isotherm is the best-fitted isotherm. Cu(II) adsorption on TON was pH-dependent. The optimal pH value for Cu (II) adsorption onto TON was 4.5 (for an initial concentration of Cu(II) of 0,283 mmol L^{-1}). The study of the effect of temperature on the adsorption kinetics allowed deducing that it was an endothermic process.

Keywords: Copper (II); Titanium oxide nanotubes; Hydrothermal treatment; Adsorption; kinetics; Thermodynamic.

1. Introduction

Copper is an essential nutrient that is required by all living organisms in very small amounts. It is found in various cells and tissues and as a cofactor and structural component of numerous metalloenzymes [1,2]. However, excessive exposure is of concern and can produce adverse health consequences [1]. Indeed, the consumption of water that contains copper (II) at concentrations more than the permissible level over many years could cause liver and kidney damage, stomach and intestinal distress, and anemia [2,3,4]. Discharge of copper (II) to the environment increases because of human activity. As it is not biodegradable [5], it can accumulate and eventually reach significant levels [6,7]. Many industrial effluents, which contain different copper derivatives, are continuously discharged to the ecosystem and significantly impact the aquatic environment. Copper-containing wastewater is waste products of various chemical industries, including mining operation, smelting, semiconductors, metallurgical, extracting and finishing processes, electroplating, refining process, batteries, electronic manufacturing, paint industry, and poultry manures [2,8].

Over the past few years, the removal of Cu (II) from wastewater has been the subject of many studies [9-12]. Several processes have been developed and used, such as chemical precipitation, ionic exchange, membrane filtration, electrochemical methods, reverse osmosis, photocatalysis, and adsorption [13-15]. Among these processes, adsorption is a fast, inexpensive, and universal method [16]. It appears the most attractive because of its interesting results, simplicity, reusability of the adsorbent, selectivity for specific metals, short operating times, low operating cost, and generally does not generate toxic by-products. Several adsorbent types were reviewed in the literature for copper (II) removal from water, and the most used ones are commercially activated charcoal and ion-exchange resins [17,18]. Other adsorbents derived from a natural material, polymers, biological wastes, industrial by-products, and nanomaterials have also been used [19-30].

Recently, nanomaterials attracted the interest of many researchers and have been used as adsorbents for several organic and inorganic contaminants; because they showed different advantages such as excellent mechanical and chemical stability, large pore volume structure, and high surface area [31,32]. In addition, the nanometric size of these structures leads to an increase in the proportion of atoms present on their surface, thus allowing a significant reactivity and an interesting adsorption capacity. The most used nanomaterials are carbon nanotubes, carbonaceous nanofibers, and graphene oxides-based nanomaterials, which are also used to remove Cu from aqueous samples [16,31]. Nevertheless, the metal oxides prove to be a possible alternative to the relatively high cost of these nanomaterials. They are highly selective for several cations, cost-effective, stable towards heat, and have a wide pH range [33-35]. Titanium dioxide (TiO_2) is the most studied metal oxide among these oxides; it exists in two major polymorphic forms, anatase and rutile. Since the surface area of anatase, the powder is typically greater than that of rutile, anatase is a preferred catalyst and adsorption support in many applications [9,32,35,36]. Among the various morphologies of Titania nanoparticles (nanowire, nanoflower, nanorod, and nanoparticles), nanotubes have the most surface area [8,13,15,37-39].

Furthermore, their high pore volume and ion-exchange capacity make them materials of great potential as effective adsorbents to metals. The removal of a variety of species such as Cu (II), Cd (II), Pb (II), Cd (II), Cr (III), or Pd (II) using titanate nanotubes has been previously investigated [40-42]. Several previous works have studied the adsorption of copper (II) on nanostructured TiO_2 in solution and powders [8,9,13,15,43,44]. Zhou et al. [13] reported that the particle size of TiO_2 nanoparticles has a strong influence on copper (II) growth on the catalyst surface. They reported that the Cu (II) adsorption was enhanced in the presence of UV irradiation. Liu et al. [43] used hydrogenated nanotubes for Cu (II) ions' adsorptive removal from aqueous solutions.

This research aimed to study the effect of pH, time, starting ion concentration, and temperature on the kinetics and mechanism of Cu (II) adsorption on titanium oxide nanotubes. Various adsorption isotherms models were also tested to assess the equilibrium data.

2. Materials

2.1. Reagents
All chemicals used in this study were of analytical grade, and all copper (II) solutions of desired concentrations were prepared by dissolving the appropriate mass of solid copper nitrate Cu $(NO_3)_2$ $3H_2O$ (Panreac Quimica S.A. brand and 99% purity) in Milli-Q water. Nitric acid was of the HPLC grade and purchased from Scharlau Chemie S.A., purity 65%. Titanium dioxide (P25, Degussa-Hüls A.G., 68% anatase and 32% rutile, S_{BET}=50 m^2. g^{-1}, non-

porous and pH_{PZC}=5.6), sodium, hydroxide (Fisher Chemicals, Purity: 98.64%), and hydrochloric acid (Panreac Quimica SA, Purity: 37%) were used for the elaboration of the TiO_2 nanotubes.

2.2. Equipment
Cu cations were analyzed using an atomic absorption spectrometer SAA type Analytik Jena "novAA 400" Model, equipped with a copper hollow cathode lamp operating at 15 mA. The wavelength was set at 324.8 nm, the pump speed was 22 rpm, and the generator power was maintained at 40.68 MHz. The nebulizer uptake rate was adjusted to give the optimum response for conventional sample introduction, pressure and flow rate of the nebulizer were 3 bars and 0.45 L min^{-1}, respectively.

2.3. Elaboration and characterization of titanium oxide nanotubes
As described in previous studies, [37,39] were used to prepare the titanate nanotubes. The elaborated material, the hydrogenated nanotubes (HNT), was calcined at 500°C for two hours in an air atmosphere to obtain titanium oxide nanotubes (TON). These later were used as adsorbents for Cu (II) removal from water samples. X-ray diffraction (XRD) studied the change in the crystal structure from the starting P25 powder to one-dimensional TON structures was studied by X-ray-diffraction (XRD). The effect of calcination temperature on the pore size distribution, mesoporous volume, and surface area has been investigated using The Brunauer-Emmett-Teller (BET) method. Changes in the morphology of the nanotubes with the calcination temperature were followed using TEM and HR-TEM (High-Resolution TEM) analysis. Comparable results were well described in previous studies [37,39]. XRD analysis of TON nanotubes showed characteristic peaks of anatase phase TiO_2 with traces of $H_{1.2}Na_{0.8}O_7Ti_3$ crystallizing in the monoclinic system. The specific surface area (S_{BET}), pore volume (V_p) as well as average diameter (dp) of TON were determined. When TiO_2 particles (P25) were transformed into hydrogenated nanotubes HNT, we noticed a considerable increase in the specific surface area from 50 to 269 m^2 g^{-1}. This can be explained by the elaborated nanotubes' multiwalled structure, which gives them a high S_{BET} since nitrogen molecules can intercalate in the inter-foliar spaces [45,46]. After calcination of HNT, a remarkable decrease in the specific surface of the TON was observed (100 m^2 g^{-1}). This decrease was accompanied by an insignificant decrease in the mesoporous volume (from 0.67 to 0.63 cm^3 g^{-1}) and an increase in pore diameter (from 9 to 23 nm). The decrease in the S_{BET} after calcination can be explained by: (i) the disappearance of the multiwalled structure of the nanotubes after calcination, thus the measured area relates only to the inner and outer surface of the nanotubes. (ii) The decrease of the number of nanotubes after calcination. The analysis of TON nanotubes by the TEM and HR-MET showed their

hollow and homogeneous nano-tubular structure. The external diameters of the nanotubes do not exceed 20 nm, while their internal diameters range between 5 and 7 nm. The point of zero charge (pH$_{pzc}$), was measured by the salt method [37,39,47], determined pH$_{pzc}$ value was about 8.3 for TON. This value shows that the surface charge is positive for a pH < 8.3 and negative for a pH > 8.3. In this work, the adsorption of copper (II) was more pronounced in the case of positive surface charges of the material, so at pH of the medium < pH$_{pzc}$.

2.4. Adsorption kinetics of Cu (II) on TON
The adsorption kinetics of Cu (II) cations on TON was determined by measuring the Cu (II) concentration change in the TON solution over time. Briefly, 50 mL of Cu (II) solution was added to 0.2 g of TON, and the material suspension was subsequently stirred at a constant temperature. At different times, 2 mL of the solution was removed, and centrifuged for 20 minutes at 5000 rpm. To determine the instantaneous concentration (C_t) of the Cu (II) cations, the recovered supernatant was analyzed by flame atomic absorption spectrometry (SAA-F). The initial concentrations of Cu (II) cations ranged from 0.041 to 6.208 mmol L^{-1}, and manipulations took place at initial pH values ranging from 4.7 to 5.4. The negative test (without TON) was conducted to ensure that the adsorption capacity was due solely to the adsorbent and did not involve the container walls. The results

obtained showed that the adsorption of copper (II) on the glass is negligible over time, and the percentage of adsorption determined up to 90 min of reaction does not exceed 5.5%.

The adsorptive uptake (Qt, mmol g^{-1}) of Cu cations by NOT, for anytime t, was determined by the difference between the initial and final ion concentrations. It is expressed by the following Equation 1:

$$Q_t = \frac{V(C_0 - C_t)}{m} \tag{1}$$

And to determine the percentage of Cu adsorption, the following Equation 2 is used:

$$R\% = \frac{(C_0 - C_t)}{C_0} \times 100 \tag{2}$$

Where: C_0 and C_t are concentrations of Cu(II) in the solution at $t = 0$ and any t, V is the volume of the solution (L), and m is the weight (g) of TON.

Different models (intraparticle diffusion model and models based on the composition of the media) [48,49] have been used to describe the mechanism of Cu(II) adsorption kinetics on TON. The equations of these models are grouped in Table 1. The variables Qe and Qt indexed in Table 1 are the amounts (mmol g^{-1}) of Cu ions adsorbed on the TON at equilibrium and time t. K$_i$, K$_0$, K'$_1$, K'$_2$, K$_1$, and K$_2$ represent the constant of kinetics cited in Table 1.

Table 1. Kinetic models used to describe the mechanism of adsorption of Cu(II) on TON.

Kinetic models		
Intraparticle diffusion model	$Q_t = K_i t^{1/2} + C$	(3)
Models based on the composition of the media $$V = \frac{dQ_t}{dt} = KQ_t{}^{\alpha}$$	*zero-order model $$V = \frac{dQ_t}{dt} = K_0$$	(4)
	* First-order model $Ln(Q_t) = K'_1 t$	(5)
	* Second-order model $$\frac{1}{Q_t} = K'_2 t$$	(6)
	* Pseudo-first-order model $Ln(Q_e - Q_t) = Ln(Q_e) - K_1 t$	(7)
	* Pseudo-second-order model $$\frac{t}{Q_t} = \left(\frac{1}{K_2 Q_e{}^2}\right) + (\frac{t}{Q_e})$$	(8)

To study the effect of pH, a volume of 50 mL of Cu(II) solution (6.208 mmol L^{-1}) was prepared, and then the pH values were adjusted with a 10^{-1} mol L^{-1} HCl or NaOH solutions. The pH range studied was between 2 and 6. 0.2 g of the material was subsequently added, and the stopwatch is started, and the equilibrium time is established (4 h).

The effect of the quantity of the adsorbent was determined for TON masses ranging from 0.1 to 0.3 g and Cu(II) solution concentrations of 0.414, 4.139,

and 6.208 mmol L^{-1}. The volume and the pH of the solution were kept constant.

The temperature effect was studied at 273, 275, 295, and 313 K. It was performed with 0.2 g of TON mixed with 50 mL of Cu(II) solution (3.311 mmol L^{-1}). The pH of the solution was kept constant.

2.5. Adsorption isotherms
Adsorption isotherm experiments were conducted, leading to the equilibrium of TiO$_2$ nanotubes (0.2 g) in contact with Cu(II) cations of concentration from

0.041 to 6.208 mmol L^{-1}. This solution was shacked and kept at different temperatures ranging from 275 to 313K. The amounts of the Cu cations adsorbed by TON were calculated by using Equation 9.

$$Q_e = (C_0 - C_e) \, V/M \qquad (9)$$

Where: Q_e (mmol g^{-1}) is the equilibrium adsorption capacity, C_0 and C_e are the initial and equilibrium concentration (mmol L^{-1}) of Cu(II) ions in solution, V (L) is the volume, and m (g) is the weight of the adsorbent.

3. Results and Discussion

3.1. Effect of temperature and thermodynamics study

Temperature is the main parameter that plays a vital role in any adsorption process [50,51]. According to Ramesh et al. [52], the temperature is one parameter that most affects the adsorption process. Therefore, we studied the kinetics of adsorption of Cu (II) ions on TON at the temperatures of 273, 275, 295, and 313 K for an initial concentration of Cu (II) equal to 3.311 mmol L^{-1}. Observed results (Table 2) showed that Adsorption capacity increases with the temperature and that the Cu(II) adsorption on TON showed an endothermic process.

Table 2. Adsorption capacity of Cu(II) ions on TON at different temperatures and calculated thermodynamic parameters.

Temperature (K)	Adsorption capacity Q_e (mmol g^{-1})	$\Delta G°$ (kJ mol^{-1})	$\Delta H°$ (kJ mol^{-1})	$\Delta S°$ (J mol^{-1}K^{-1})
273	0.8271	-12.749		
275	0.8272	-13.115	37.1685	182.8498
295	0.8252	-16.772		
313	0.8275	-20.063		

Our results agree with many authors who reported that the main reason was that the active site increases with increasing temperature due to the endothermic nature of the process. In addition, the adsorbent's intra-particle diffusion increased with the adsorption temperature [50,53]. According to Rashidi et al. [54], this increase means that the adsorption process was endothermic due to the increased mobility of metal ions and their tendency to adsorb to the adsorbent's surface to the more significant activity of binding sites as the temperature increases

Thermodynamic parameters: the standard free energy ($\Delta G°$), enthalpy change ($\Delta H°$), and entropy change ($\Delta S°$) were determined using the following equations (10-13).

$$K_d = \frac{Qe}{Ce} \qquad (10)$$

$$Ln \, K_d = \frac{\Delta S^0}{R} - \frac{\Delta H^0}{RT} \qquad (11)$$

$$\Delta G^0 = -RT \, LnK_d \qquad (12)$$

$$\Delta G^0 = \Delta H^0 - T\Delta S^0 \qquad (13)$$

where: R is the universal gas constant (8.314 J mol^{-1} K^{-1}), T is the temperature expressed in Kelvin and K_d is the thermodynamic equilibrium constant for the adsorption process, determined by plotting ln q_e /C_e versus q_e and extrapolating to zero q_e [55,56]. $\Delta H°$ and $\Delta S°$ were obtained from the slope of the straight line and the intercept of the graph, respectively. As presented in Table 2, the free energy of the process ($\Delta G°$) for Cu(II) decreased slightly from 273 to 313 K. Negative $\Delta G°$ means that the adsorption

process is spontaneous and more favorable at higher temperatures. When the ions approach the particle surface, some of the water molecules forming the hydration shell of ions are stripped off. Simultaneously, the degree of freedom of Cu(II) ions declines [57]. The $\Delta S°$ value is positive, indicating high randomness at the solid/liquid phase with structural changes in the adsorbate and the adsorbent. This could be possible because the mobility of adsorbate ions/molecules in the solution increases with increasing temperature. Meanwhile, the value of $\Delta H°$ is positive, meaning that the adsorption process is an endothermic reaction, which supports the influence of temperature on adsorption property [58,59].

3.2. Effect of contact time on the adsorption capacity of Cu(II) on TON

The kinetic study was essential to an adsorption process because it demonstrated the elimination rate of Cu(II) and controlled the residual time of the whole adsorption process. The adsorption kinetic depends on many factors, and to describe it, it is necessary to consider the limiting step in the process. The study of the efficiency of TON as adsorbents of Cu(II) ions requires the drawing of curves giving the variation of the adsorbed quantity Q_t as a function of time for different initial Cu (II) concentrations.

After analyzing the results presented in Figure 1 (for low initial concentrations varying between 0.041 and 0.414 mmol L^{-1}), the adsorption kinetics showed instantaneous adsorption and was concentration-dependent.
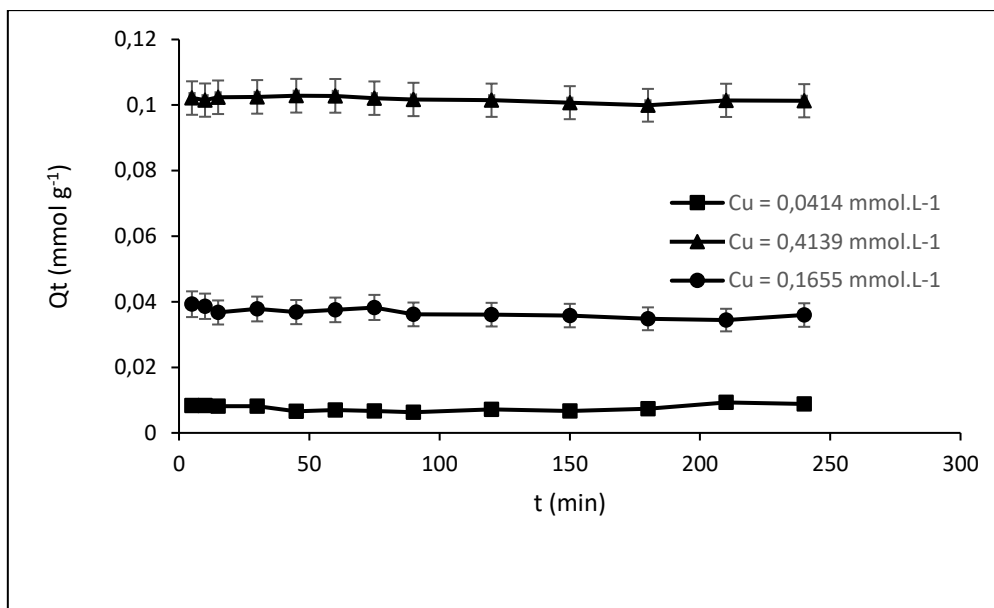
Figure 1. Adsorption kinetics for low Cu(II) concentrations. Volume of solution=50 mL; mass of TON = 0.2 g; T=25°C

An increase in adsorption capacity has been reported to increase the initial concentration of Cu ions. This is because adsorption on adsorbents is a diffusion-based process [58].

Figure 2 provides the results of the time equilibrium studies for the adsorption of Cu onto TON at high initial concentrations (3.311, 4.139, and 6.208 mmol L^{-1}).
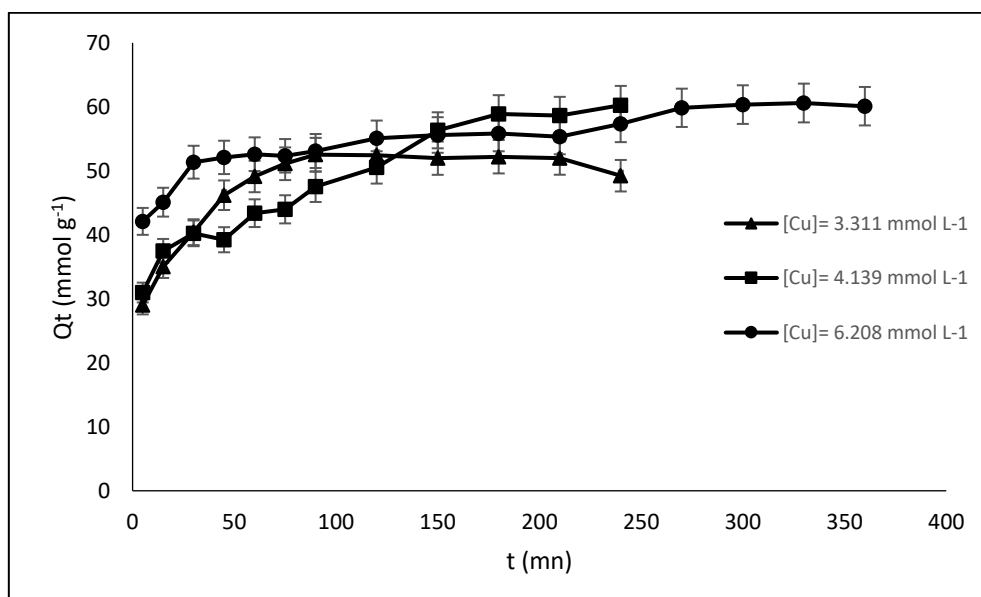
Figure 2. Adsorption kinetics for high Cu (II) concentrations. Volume of Cu=50 mL; mass of TON = 0.2 g; T=25°C

The results show clearly that the percentage of absorption is important at high concentrations even if an equilibrium is reached more slowly (40 min). The Amount of Cu adsorbed at equilibrium (Q_e) is almost the same for all the initial Cu(II) concentrations studied, probably due to saturation of the adsorbent sites. Many authors considered this behavior due to physical adsorption [58,60].

3.3. Effect of initial concentration

The initial concentration of metal ions is a significant parameter influencing the adsorption performance. The adsorption isotherm is obtained by plotting the variation of the amount adsorbed at equilibrium (Q_e) as a function of the Cu(II) concentration at the equilibrium (C_e). According to Figure 3, the amount of Cu(II) adsorbed (Q_e) increases rapidly for low concentrations in solution (0.414 to 4.552 mmol L^{-1}), until it tends to be a constant with the increasing initial concentration. This constant is the maximum

adsorption capacity that the adsorption isotherm models can calculate. According to Li et al. [61] and Rahman et al. [62], metals are absorbed by specific sites at low concentration values. In contrast, the specific sites are saturated with increasing metal concentration and filling exchange sites.
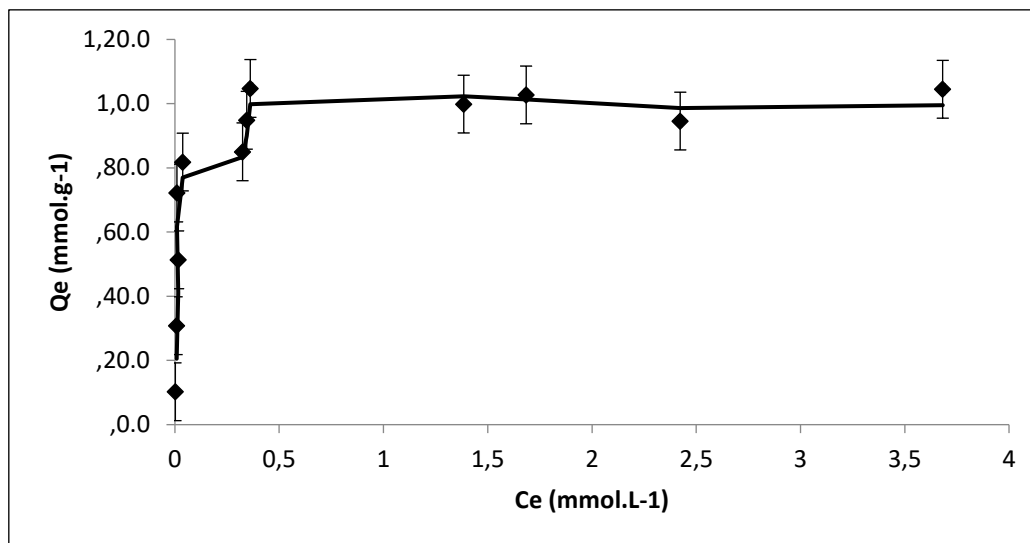
Figure 3. Adsorption isotherm of Cu (II) cations by TON. Volume of solution=50 mL; mass of TON = 0.2 g; T=25°C.

3.4. Modeling adsorption isotherm

Langmuir model

The Langmuir model is based on the following assumptions: the formation of a single layer of adsorbate on the surface of the adsorbent, the adsorbed sites are energetically identical, and the surface is homogeneous with no interaction between the adsorbed molecules [58,63]. The Langmuir Equation 14:

$$Q_e = Q_m \left(\frac{b\, C_e}{1 + b\, C_e} \right) \tag{14}$$

Where: Q_m: adsorption capacity at saturation, characteristic of the monolayer formation of adsorbed molecules and expressed in mmol g^{-1}, b: equilibrium constant characteristic of the adsorbent depending on the temperature and the experimental conditions, expressed in L mmol^{-1}.

The modeling of the adsorption isotherm of Cu(II) cations on TON by the Langmuir model was carried out based on the following linearized form Equation 15:

$$\frac{C_e}{Q_e} = \frac{1}{Q_m\, b} + \frac{C_e}{Q_m} \tag{15}$$

Freundlich model

The Freundlich model is based on an empirical equation that translates the variation of energies with the quantity adsorbed. It is used in the case of the formation of several successive adsorption layers on the surface and when heterogeneous sites with different binding energies are involved. Moreover, this model admits the existence of interactions between the adsorbed molecules. The Freundlich Equation 16 is written in the following form:

$$Q_e = K_F\, C_e^{\frac{1}{n}} \tag{16}$$

K_F: adsorbent capacity (mmol g^{-1} (mmol L^{-1})$^{-1/n}$), 1/n: heterogeneity factor. The modeling of the adsorption isotherm of Cu (II) cations by TON according to the Freundlich model

was carried out based on the empirical Equation 17:

$$\mathrm{Ln}\, Q_e = \mathrm{Ln}\, K_F + \frac{1}{n} \mathrm{Ln}\, C_e \tag{17}$$

Table 3. Langmuir and Freundlich isotherm parameters for the adsorption of Cu(II) ions on TON.

Isotherm models	Parameters	
Langmuir	R^2	0.9972
	Q_m (mmol g^{-1})	1.0215
	b (L mmol^{-1})	39.2538
Freundlich	R^2	0.6166
	n	4.6317
	K_f (mmol g^{-1} (mmol L^{-1})$^{-1/n}$)	1.0058

In order to identify the isotherm that best represents the adsorption of the Cu(II) cations on the TON adsorbent, the experimental data obtained were applied to the two models, Freundlich and Langmuir. The parameters of the isotherm models are summarized in Table 3.

The regression coefficients of the Langmuir model (0.9972) are greater than that of the Freundlich model (0.6166). According to the obtained result, linearization was obtained in the whole range of the studied concentrations for the Langmuir model. Consequently, this latter better explains the Cu(II)

adsorption data and suggests that adsorption is a monolayer type [50,58,64].

3.5. Modeling adsorption kinetics

To perform the adsorption process at a larger scale, the kinetic parameters should be determined. Therefore, the kinetic adsorption data have been simulated with five models: the intraparticle diffusion model, the first-order model, the second-order model, the pseudo-first-order model, and the pseudo-second-order model. The kinetic parameters of these models were determined, and the results are presented in Table 4.

Table 4. Kinetic parameters for the adsorption of Cu(II) ions by TiO_2 nanotubes TON.

Kinetics models	Parameters						
	Initial concentration						
		0.041	0.165	0.414	3.310	4.138	6.208
Intraparticle diffusion	R^2	0.0007	0.7075	0.3932	0.7759	0.8774	0.8992
	K_d (mmol g^{-1} min$^{-1/2}$)	6 E-0.6	-0.0003	-0.0001	0.0554	0.0609	0.0148
	C	0.0076	0.0392	0.1028	0.1684	0.1364	0.6867
First order	R^2	0.0322	0.6737	0.4473	0.0024	0.0748	0.7498
	K_1 (min^{-1})	0.0003	-0.0004	-7E-	0.0001	0.0008	0.0007
Second order	R^2	0.0245	0.6778	0.4468	0.0951	0.0515	0.7008
	K_2 (mmol^{-1} g min^{-1})	-0.033	0.0112	0.0007	0.0026	0.0019	-0.0009
Pseudo-first order	R^2	0.7901	0.3416	0.494	0.6695	0.9325	0.0832
	K'_1 (min^{-1})	0.0689	0.02	-	0.0205	0.0168	-0.0026
	Q_{e1} (mmol g^{-1})	0.5412	0.0586	0.0005	0.4623	0.7482	0.1003
Pseudo-second order	R^2	0.9566	0.9988	0.9999	0.9974	0.9837	0.9976
	K'_2 (g mol^{-1} min^{-1})	5.6042E-8	-1.9 .10^{-5}	-	0.2673	0.0820	0.0897
	Q_{e2} (mmol g^{-1})	0.0085	0.0349	0.1008	0.8124	0.943	0.9625

From the values of the correlation coefficient R^2, the kinetic adsorption of Cu (II) can be best fitted by the semi-empirical kinetic model, the pseudo-second-order, for all initial concentrations. It represents the

best correlation coefficient (R^2) closest to 1 (Figure 4). Similar results were also observed in many studies [50, 62].
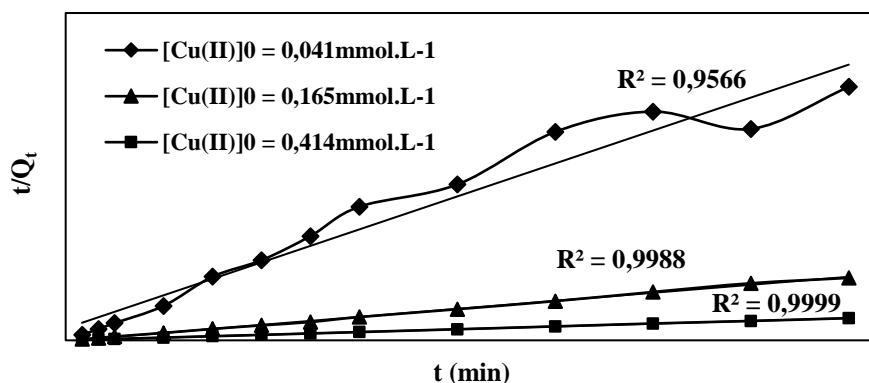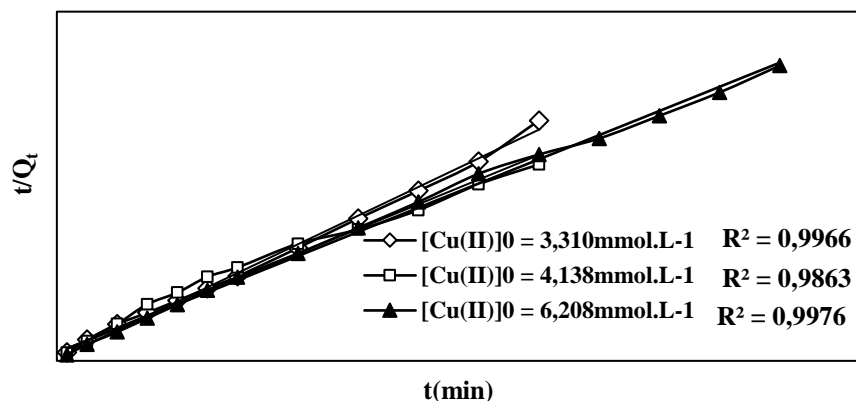
Figure 4. Pseudo-second-order model of adsorption kinetics for low and high Cu (II) concentrations
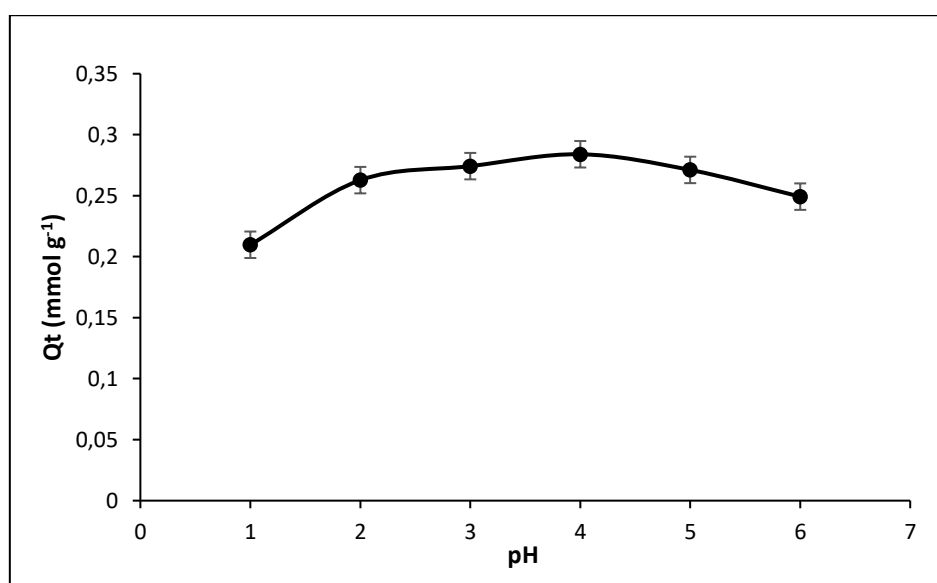
Figure 5. Effect of pH on Cu(II) yield adsorption. $[Cu(II)]_0$=6,211mmol/L; Volume of solution=50 mL; mass of TON=0.2 g

3.6. Effect of pH

The effect of pH on Cu(II) adsorption on TON at initial pH values ranging between 2 and 6 is shown in Figure 5. The results show that Cu(II) adsorption is strongly influenced by pH. Results indicate that the adsorption capacity is low at pH values below 4, possibly due to an excess of H^+ ions competing with Cu(II) ions for the available adsorption sites [65]. This adsorption capacity reached its maximum values when the pH was between 4 and 5 (0,283 mmol L^{-1} at pH 4.5), then decreased slightly with pH values above 5. Cu cations precipitated as insoluble hydroxide [66, 67]. Consequently, its concentration as free cations in the solution decreases, and they do not participate in the adsorption phenomenon, which can raise the competitive adsorption of free protons in the solution. From where a slight decrease in the adsorption yield was observed. This insignificant reduction can also be due to a small phenomenon of desorption which is possible with the continuous stirring of the solution. Indeed, all manipulations were performed at pH values ranging from 4 to 5, values for which copper is present as Cu(II) cations.

3.7. Effect of the mass of adsorbent TON

The influence of the mass of adsorbent, going from 0.1 to 0.3 g while keeping the volume of the solution constant, on the efficiency of Cu(II) removal from aqueous solutions was investigated, and the results are presented in Table 5.

As can be seen, the removal efficiency increases while the mass of the adsorbent increases. In addition, for an initial concentration of Cu(II) equal to 6.208 mmol L^{-1}, the adsorption percentage varies from 60.9 to 89.9 % when the mass of the adsorbent increases from 0.2 to 0.3 g. This is explained by increasing the available surface and active sites on the surface. Therefore, we can conclude that the increase depends on the initial concentration of the metals. Likewise, many authors reported in their studies that the mass of adsorbents significantly affects the adsorption process [68,69]

Table 5. Effect of the mass of adsorbent.

$[Cu(II)]_0$ (mmol.L^{-1})	0.414			4.138			6.208		
m_{ads} (g)	C_e (mmol. L^{-1})	t_e (min)	%$_{ads}$	C_e (mmol. L^{-1})	t_e (min)	%$_{ads}$	C_e (mmol. L^{-1})	t_e (min)	%$_{ads}$
0.1	0.026	60	93.57	2.502	210	39.54	-	-	-
0.2	0.002	60	99.35	0.344	240	91.67	2.423	360	60.96
0.3	-	-	-	-	-	-	0.628	360	89.88

3.8. Comparative study

A comparative study of the kinetic behavior of Cu (II) cation adsorption on hydogenotitanate nanotubes (HNT), titanium oxide nanotubes (TON), and TiO$_2$ precursor (P25) was performed with an initial Cu (II) concentration of 4.138 mmol L^{-1}. P25 is a model material with good purity and insolubility in water [70].

According to the results obtained in Figure 6, the best adsorption kinetics was observed with TON. Indeed, a maximum of adsorption (higher than 95%) was reached after 120 min, while HNT allowed to reach a percentage of 76.89%. However, the amount of Cu (II) cations adsorbed by P25 was meager; it was about 1.9% after a contact time of 240 min.
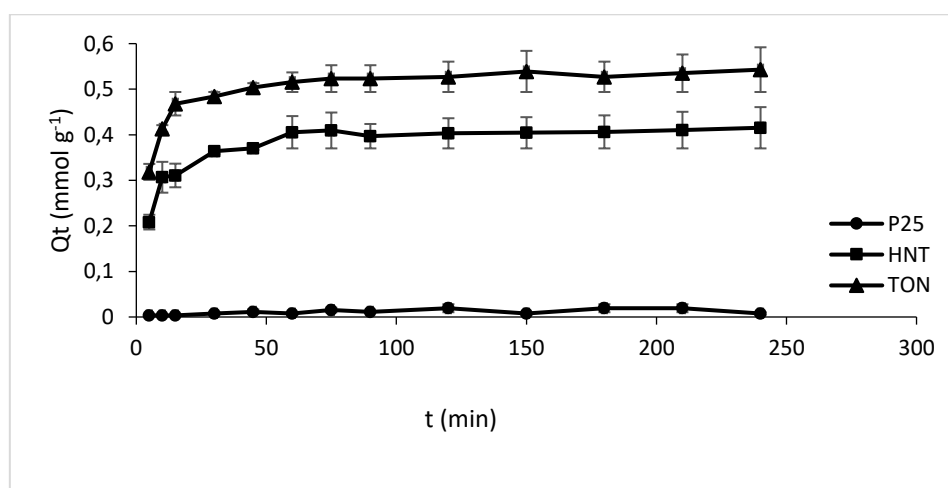
Figure 6. Adsorption kinetics of Cu (II) on P25 TiO$_2$, NHT, and TON. $[Cu]_0$=4.140 mmol L^{-1}; Volume of solution=50 mL; Mass of adsorbent=0.2 g; T= 25 °C

4. Conclusion

This study indicates that titanium oxide nanotubes, with a specific surface area of about 100 m^2 g^{-1}, had shown an exciting adsorption capacity of copper (II) ions. At low Cu(II) concentration, maximum adsorption was reached instantly. The adsorption reaction was thus swift. Strong adsorption was also obtained at high copper (II) concentrations, even with slower reaction kinetics. Cu(II) adsorption processes are closely related to temperature, adsorption time, initial Cu(II) concentration, and pH. The adsorption conforms to the pseudo-second-order kinetic model and follows Langmuir isotherm models. The increase of adsorption in the temperature range 273–313 K means that the adsorption process of copper (II) ions by TON was endothermic. Titanium oxide nanotubes

placed in an aqueous solution (pH between 4 and 5 lower than pH$_{pzc}$ = 8.3) become positively charged. When this material was brought into contact with a solution containing Cu(II) cations, an exchange between the proper cations of TON and the Cu(II) ions in the solution can take place. So, the adsorption of Cu cations in TON was physisorption. It can be wholly desorbed by other competitive cations or a suitable solvent. Equilibrium of distribution of the two ions in the two phases was reached:

$$\vdash A + B^+ == \vdash B + A^+$$
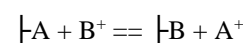
Where: $\vdash A$: the proper cations of TON (H$^+$, Na$^+$); B$^+$ and A$^+$: cations in solutions.

Significantly, this study shows that even small amounts of titanium oxide nanotubes are enough to

enhance the adsorption potential of the Cu(II) cations in terms of the adsorption rate and capacity.

Conflict of Interest

The authors declare that the research was conducted without any commercial or financial relationships that could be construed as a potential conflict of interest.

References

1- L.M. Gaetke, C.K. Chow, Copper toxicity, oxidative stress, and antioxidant nutrients, Toxicology, **2003**, 189, 147-163.

2- I. Blanco-Penedo, M.J. Cruz, M. López-Alonso, M. Miranda, C. Castillo, J. Hernández, J.L. Benedito, Influence of copper status on the accumulation of toxic and essential metals in cattle, Environment International, **2006**, 32, 901-906.

3- R.S. Bonnie, Essentiality and Toxicity in Copper Health Risk Assessment: Overview, Update and Regulatory Considerations, Journal of Toxicology and Environmental Health, Part A: Current Issues, **2010**, 73:2-3 114-127.

4- O.H. Valeria, L. Glendy, B. Qais, J.A. Field, S.A. Reyes, Toxicity of copper (II) ions to microorganisms in biological wastewater treatment systems, Science of the Total Environment, **2015**, 411, 380–385.

5- H. Ali, E. Khan, I. Ilahi, Environmental chemistry and ecotoxicology of hazardous heavy metals: environmental persistence, toxicity, and bioaccumulation, Journal of Chemistry, **2019**, 2019, 14.

6- M.A. Barakat, New trends in removing heavy metals from industrial wastewater, Arabian Journal of Chemistry, **2011**, 4, 361–377.

7- N. Herawati, S. Suzuki, K. Hayashi, IF. Rivai, H. Koyama, Cadmium, copper, and zinc levels in rice and soil of Japan, Indonesia, and China by soil type, Bulletin of environmental contamination and toxicology, **2000**, 64, 33-39.

8- M.A. Barakat, Adsorption behavior of copper and cyanide ions at TiO_2–solution interface, Journal of colloid and interface science, **2005**, 291, 345-352.

9- D. Vu, Z. Li, H. Zhang, W. Wang, Z. Wang, X. Xu, C.Wang, Adsorption of Cu(II) from aqueous solution by anatase mesoporous TiO_2 nanofibers prepared via electrospinning, Journal of Colloid and Interface Science, **2012**, 367, 429–435.

10- J. Mittal, R. Ahmad, A. Mariyam, V.K. Gupta, Alok Mittal, Expeditious and enhanced removal of heavy metal from aqueous environment by carica papaya peel carbon (PPC): a green and low-cost adsorbent, Desalination and Water Treatment, **2021**, 210, 365-376.

11- R. Ahmad, A. Mirza, Application of Xanthan gum/ n-acetyl cysteine modified mica bionanocomposite as an adsorbent for the removal of toxic heavy metals, Groundwater for Sustainable Development, **2018**, 7, 101-108.

12- R. Ahmad, A. Mirza, Inulin-follic-acid/bentonite: A novel nanocomposite for confiscation of Cu (II) from synthetic and industrial wastewater, Journal of Molecular Liquids, **2017**, 241, 489-499.

13- Q.X. Zhou, X.N. Zhao, J.P. Xiao, Preconcentration of nickel and cadmium by TiO_2 nanotubes as solid-phase extraction adsorbents coupled with flame atomic absorption spectrometry, Talanta, **2009**, 77, 1774-1777.

14- S.A. Al-Saydeh, M.H. El-Naas, S.J. Zaidi, Copper removal from industrial wastewater: A comprehensive review, Journal of Industrial and Engineering Chemistry, **2017**, 56, 35-44.

15- X.N. Zhao, Q.Z. Shi, G.H. Xie, Q.X. Zhou, TiO_2 nanotubes: A novel solid-phase extraction adsorbent for the sensitive determination of nickel in environmental water samples, Chinese Chemical Letters, **2008**, 19, 865-867.

16- I. Anastopoulos, A. Mittal, M. Usman, Y. Mittal, G. Yu, A. Núñez-Delgadofez, M. Kornaros, review on halloysite-based adsorbents to remove pollutants in water and wastewater, J. Mol. Liq., **2018**, 269, 855–868.

17- R.C. Bansal, M. Goyal, Activated Carbon Adsorption, CRC Press Taylor & Francis Group: Boca Raton, FL, USA, **2005**.

18- S.A. Al-Saydeh, M.H. El-Naas, S.J. Zaidi, Copper removal from industrial wastewater: A comprehensive review, Journal of Industrial and Engineering Chemistry, **2017**, 56, 35-44.

19- R. Ahmad, I. Hasan, L-Mthionine Montmorillnite Encapsulateed Guar Gum-g-Polyacrylonitrile Copolymer Hybrid nanocomposite for removal of heavy metals, Groundwater for Sustainable Development, **2017**, 5, 75-84.

20- R. Ahmad, A. Mirza, Adsorption of Pb (II) and Cu (II) by alginate – Au- Mica bionanocomposite: Kinetic, isotherms and thermodyna-mic studies, Process Safety and Environmental Protection, **2017**, 109, 1-10.

21- R. Ahmad, I. Hasan, L-cystein modified bentonite-cellulose nanocomposite (cellu/cys-bent) for the adsorption of Cu^{2+}, Pb^{2+} and Cd^{2+} ions from aqueous solution, Journal of Separation Science and Technology, **2016**, 51, 381-394.

22- A. Mittal, R. Ahmad, I. Hasan, Biosorption of Pb^{2+}, Ni^{2+} and Cu^{2+} ions from aqueous solutions by L-cystein modified Montmorillonite nanoclay/ Sodium Alginate (Alg/cys-MMT) bio-nanocomposite, Journal of Desalination and Water Treatment, **2016**, 57, 17790-17807.

23- A. Mittal, R. Ahmad, I. Hasan, Poly (methyl methacrylate)-grafted alginate/Fe_3O_4 nanocomposite: synthesis and its application for the removal of heavy metal ions, Journal of Desalination and Water Treatment, **2016**, 57, 19820-19833.

24- R. Ahmad, S. Haseeb, Competitive adsorption of Cu^{2+} and Ni^{2+} on Luffaacutangula modified

Tetraethoxysilane (LAP-TS) from the aqueous solution: Thermodynamic and isotherm studies, Groundwater for Sustainable Development, **2015**, 2, 146-154.

25- R. Ahmad, S. Haseeb, Absorptive removal of Pb^{2+}, Cu^{2+} and Ni^{2+} from the aqueous solution by using Ground Nut Husk Modified with Guar Gum (GG): Kinetic and Thermodynamic Studies, Groundwater for Sustainable Development, **2015**, 1, 41-49.

26- R. Ahmad, S. Haseeb, Black Cumin Seed (BCS)– a non-conventional adsorbent for the removal of Cu (II) from aqueous solution, Journal of Desalination and Water Treatment, **2015**, 56, 2512-2521.

27- R. Kumar, M. Kumar, R. Ahmad, M.A. Barakat, L-Methionine modified Dowex-50 ion-exchanger of reduced size for the separation and removal of Cu (II) and Ni (II) from aqueous solution, Chemical Engineering Journal, **2013**, 218, 32-38.

28- R. Ahmad, S. Haseeb, Adsorption of Cu^{2+} from aqueous solution onto agricultural solid waste-mentha: characterization, isotherms and kinetic studies, Journal of Dispersion Science and Technology, **2012**, 33, 1188-1196.

29- R. Ahmad, R. Kumar, S. Haseeb, Adsorption of Cu^{2+} from aqueous solution onto iron oxide coated eggshell powder: Evaluation of equilibrium, isotherms, kinetics, and regeneration capacity, Arabian Journal of Chemistry, **2012**, 5, 353-359.

30- S. Mustapha, D.T. Shuaib, M.M. Ndamitso, Adsorption isotherm, kinetic and thermodynamic studies for the removal of Pb(II), Cd(II), Zn(II) and Cu(II) ions from aqueous solutions using Albizia lebbeck pods, Appl Water Sci., **2019**, 9,142.

31- X. Ren, C. Chen, M. Nagatsu, X. Wang, Carbon nanotubes as adsorbents in environmental pollution management: A review, Chem. Eng. J., **2011**, 170, 395–410.

32- U. Diebold, The surface science of titanium dioxide, Surface Science Reports, **2003**, 48, 53-229.

33- A.A. Ismail, A.A. El-Midany, I.A. Ibrahim, H. Matsunaga, Heavy metal removal using SiO_2–TiO_2 binary oxide: experimental design approach, Adsorption, **2008**, 14, 21-29.

34- S. Mustapha, M.M. Ndamitso, A.S. Abdulkareem, J.O. Tijani, D.T. Shuaib, A.O. Ajala, A.K. Mohammed, Application of TiO_2 and ZnO nanoparticles immobilized on clay in wastewater treatment: a review, Appl. Water Sci., **2020**, 10, 49.

35- V.E. Henrich, P.A. Cox, The Surface Science of Metal Oxides, Cambridge Univ. Press, Cambridge, UK, **1994**.

36- S. Mustapha, J.O. Tijani, M.M. Ndamitso, A.S. Abdulkareem, D.T. Shuaib, A.T. Amigun, H.L. Abubakar, Facile synthesis and characterization of TiO_2 nanoparticles: X-ray peak profile

analysis using Williamson–Hall and Debye–Scherrer methods, Int. Nano. Lett., **2021**, 11, 241-261.

37- B. Kefi, B. Bouchmila, I. Martin, N. M'Hamdi, Titanium Dioxide Nanotubes as Solid-Phase Extraction Adsorbent for the Determination of Copper in Natural Water Samples, Materials, **2022**, 15, 822.

38- H. Niu, Y. Cai, Y. Shi, F. Wei, S. Mou, G. Jiang, Cetyltrimethylammonium bromide-coated titanate nanotubes for solid-phase extraction of phthalate esters from natural waters prior to high-performance liquid chromatography analysis, Journal of Chromatography A, **2007**, 1172, 113-120.

39- B. Bejaoui, L. Elatrache, H. Kochkar, A. Ghorbel, TiO_2 Nanotubes as Adsorbent for the Solid Phase Extraction of Polycyclic Aromatic Hydrocarbons from Environmental Water Samples, Journal of Environmental Sciences, **2011**, 23, 860-867.

40- G. Sheng, S. Yang, J. Sheng, D. Zhao, X. Wang, Influence of solution chemistry on the removal of Ni(II) from aqueous solution to titanate nanotubes, Chemical Engineering Journal, **2011**, 168, 178-182.

41- R. Saleh, A.H. Zaki, F.I. Abo El-Ela, A.A. Farghali, M. Taha, R. Mahmod, Consecutive removal of heavy metals and dyes by a fascinating method using titanate nanotubes, Journal of Environmental Chemical Engineering, **2021**, 9, 104726.

42- L. Xiong, C. Chen, Q. Chen, J. Ni, Adsorption of Pb(II) and Cd(II) from aqueous solutions using titanate nanotubes prepared via hydrothermal method, Journal of Hazardous Materials, **2011**, 189, 741-748.

43- S.S. Liu, C.K. Lee, H.C. Chen, C.C. Wang, L.C. Juang, Application of titanate nanotubes for Cu (II) ions adsorptive removal from aqueous solution, Chemical Engineering Journal, **2009**, 147,188-193.

44- F. Rashidi, R.S. Sarabi, Z. Ghasemi, A. Seif, Kinetic, equilibrium and thermodynamic studies for the removal of lead (II) and copper (II) ions from aqueous solutions by nanocrystalline TiO_2, Superlattices and Microstructures, **2010**, 48, 577-591.

45- G. Kamińska, M. Dudziak, E. Kudlek, J. Bohdziewicz, Preparation, Characterization, and Adsorption Potential of Grainy Halloysite-CNT Composites for Anthracene Removal from Aqueous Solution, Nanomaterials, **2019**, 9, 890.

46- D. Yu, J. Wang, W. Hu, R. Guo, Preparation and controlled release behavior of halloysite/2-mercaptobenzothiazole nanocomposite with calcined halloysite as nanocontainer, Mater. Design, **2017**, 129, 103–110.

47- J.P. Brunelle, Preparation of catalysts by metallic complex adsorption on mineral oxides, Pure Appl. Chem., **1978**, 50, 1211-1229.

48- H. Qiu, L. Lv, B.C. Pan, Q.J. Zhang, W.M. Zhang, Q.X. Zhang, Critical review in adsorption kinetic models, J. Zhejiang Univ. Sci. A, **2009**, 10, 716–24.

49- J. Lin, L. Wang, Comparison between linear and non-linear forms of pseudo-first-order and pseudo-second-order adsorption kinetic models for the removal of methylene blue by activated carbon, Front Environ. Sci. Eng. China, **2009**, 3, 320–324.

50- H. Xu, W. Pei, X. Li, J. Zhang, Highly Efficient Adsorption of Phenylethanoid Glycosides on Mesoporous Carbon, Frontiers in Chemistry, **2019**, 7, 781.

51- L. Alcaraz, I. García-Díaz, F.J. Alguacil, F.A. López Gómez, Removal of copper ions from wastewater by adsorption onto a green adsorbent from winemaking wastes, BioResources, **2020**, 15, 1112-1133.

52- K. Ramesh, A. Rajappa, V. Nandhakumar, Adsorption of turquoise blue dye from aqueous solution using microwave-assisted zinc chloride activated carbon prepared from delonix regia pods, Zeitschrift für Physikalische Chemie, **2017**, 231, 1057-1076.

53- X. Peng, F. Hu, F.L.Y. Lam, Y. Wang, Z. Liu, H. Dai, Adsorption behavior and mechanisms of ciprofloxacin from aqueous solution by ordered mesoporous carbon and bamboo-based carbon, J. Colloid Interface Sci., **2015**, 460, 349–360.

54- F. Rashidi, R.S. Sarabi, Z. Ghasemi, A. Seif, Kinetic, equilibrium and thermodynamic studies for the removal of lead (II) and copper (II) ions from aqueous solutions by nanocrystalline TiO_2, Superlattice Microst., **2010**, 48, 577–591.

55- H.M. Marwani, H.M. Albishri, T.A. Jalal, E.M. Soliman, Study of isotherm and kinetic models of lanthanum adsorption on activated carbon loaded with recently synthesized Schiff's base, Arab. J. Chem., **2013**, 68, 1–9.

56- G. Zeng, C. Zhang, G. Huang, J. Yu, Q. Wang, J. Li, Adsorption behavior of bisphenol A on sediments in Xiangjiang River, central-south China, Chemosphere, **2006**, 65, 1490–9.

57- N. Ayar, B. Bilgin, G. Atun, Kinetics and equilibrium studies of the herbicide 2,4-dichlorophenoxyacetic acid adsorption on bituminous shale, Chem. Eng. J., **2008**, 138, 239–48.

58- I. Bouchmila, B. Bejaoui Kefi, R. Souissi, M. Abdellaoui, Purification, characterization, and application of cherty rocks as sorbent for separation and preconcentration of rare earth. Journal of Materials Research and Technology, **2019**, 8, 2910-2923.

59- A.A. Khan, R.P. Singh, Adsorption thermodynamics of carbofuran on Sn(IV) arsenosilicate in H^+, Na^+, and Ca^{2+} forms, Colloid Surf. A, **1987**, 24, 33–42.

60- K. Haitham, S. Razak, M.A. Nawi, kinetics and isotherm studies of methyl orange adsorption by a highly recyclable immobilized polyaniline on a glass plate, Arabian Journal of Chemistry, **2019**, 12, 1595-1606.

61- J. Li, J. Hu, G. Sheng, G. Zhao, Q. Huang, Effect of pH, ionic strength, foreign ions, and temperature on the adsorption of Cu(II) from aqueous solution to GMZ bentonite, Colloids Surf. A Physicochem. Eng. Asp., **2009**, 349, 195–201.

62- M.S. Rahman, M.R. Islam, Effects of pH on isotherms modeling for Cu(II) ions adsorption using maple wood sawdust, Chem. Eng. J., **2009**, 149, 273–280.

63- R. Saadi, Z. Saadi, R. Fazaeli, N.E. Fard, Monolayer and multilayer adsorption isotherm models for sorption from aqueous media, Korean Journal of Chemical Engineering, **2015**, 32, 787-799.

64- O. Moradi, K. Zare, M. Monajjemi, M. Yari, H. Aghaie, The Studies of Equilibrium and Thermodynamic Adsorption of Pb(II), Cd(II) and Cu(II) Ions from Aqueous Solution onto SWCNTs and SWCNT–COOH Surfaces, Fullerenes, Nanotubes and Carbon Nanostructures, **2010**, 18, 285–302.

65- A. Benhammou, A. Yaacoubi, L. Nibou, B. Tanouti, Adsorption of metal ions onto Moroccan stevensite: kinetic and isotherm studies, Journal of Colloid and Interface Science, **2005**, 282, 320–326.

66- Y. Shi, Q. Zhang, L. Feng, Q. Xiong, J. Chen, Preparation and adsorption characters of Cu(II)-imprinted chitosan/attapulgite polymer, Korean Journal of Chemical Engineering, **2014**, 31, 821–827.

67- J.K. Yang, S.M. Lee, EDTA effect on the removal of Cu(II) onto TiO_2, Journal of Colloid and Interface Science, **2005**, 282, 5–10.

68- B.A. Militaru, R. Pode, L. Lupa, W. Schmidt, A. Tekle-Röttering, N. Kazamer, Using Sewage Sludge Ash as an Efficient Adsorbent for Pb (II) and Cu (II) in Single and Binary Systems, Molecules, **2020**, 25, 2559.

69- T. Kalak, R.Cierpiszewski, Comparative studies on the adsorption of Pb(II) ions by fly ash and slag obtained from CFBC technology, Pol. J. Chem. Technol., **2019**, 21, 72–81.

70- T.P. Malini, A. Ramesh, J.A. Selvi, M. Arthanareeswari, P. Kamaraj, Kinetic Modeling of Photocatalytic Degradation of Alachlor using TiO_2 (Degussa P25) in Aqueous Solution, Oriental Journal of Chemistry, **2016**, 32, 3165.